

Bessel–Gauss resonator with internal amplitude filter

Igor A. Litvin^{a,b,*}, Andrew Forbes^{a,c,*}

^a CSIR National Laser Centre, P.O. Box 395, Pretoria 0001, South Africa

^b Laser Research Institute, University of Stellenbosch, Stellenbosch 7602, South Africa

^c School of Physics, University of KwaZulu-Natal, Private Bag X54001, Durban 4000, South Africa

Received 21 August 2007; received in revised form 18 December 2007; accepted 19 December 2007

Abstract

We investigate a conventional resonator configuration, using only spherical curvature optical elements, for the generation of Bessel–Gauss beams. This is achieved through the deployment of a suitable amplitude filter at a Fourier plane created by careful selection of the geometric cavity parameters, such as mirror curvatures and resonator length. We analyze the loss behaviour of the odd and even modes, and show that the lowest Bessel–Gauss mode does not necessarily have the lowest loss.

© 2007 Elsevier B.V. All rights reserved.

Keywords: Bessel–Gauss beams; Fox–Li; Fourier resonator; Confocal resonator

1. Introduction

Bessel beams (BBs) represent a class of so-called diffraction free solutions to the Helmholtz equation, and have been studied extensively since the seminal work of Durnin et al. in the late 1980s [1–3]. Of more practical relevance are Bessel–Gauss beams (BGBs), which are spatially-infinite BBs confined by a Gaussian envelope in the transverse spatial plane, making them spatially finite. These beams are easily generated external to the laser cavity by illuminating an axicon with a Gaussian beam, and offer a good approximation to the properties of true BBs. A recent review of BBs and BGBs as well as their applications can be found in [4].

Intra-cavity generation of BGBs has been successfully shown through various techniques using non-conventional elements. In [5] a new method was proposed for BB generation by means of a confocal resonator with an annular active medium, and an estimation of the size of the “diffraction-free” zone was presented. Axicon-based reso-

nators were independently proposed by Rogel-Salazar et al. [6] and Khilo et al. [7]. The axicon-based resonator supporting Bessel modes in [7] was composed of two plane mirrors with an axicon placed close to one of them, and it was shown that if the axicon adjacent mirror was concave, then BGBs were produced. Analytical expressions relating parameters of the resonator and characteristics of its modes were obtained and analyzed. The resonator scheme was implemented in an experiment to confirm the possibility of the generation of zero-order Bessel beams. Unstable resonators for BB generation were proposed in [8] and the use of intra-cavity phase conjugating mirrors for BGB generation was shown in [9]. More recently axicon-based BGB resonators with concave output couplers were considered [10] using both geometrical and wave optics approaches, while unstable axicon-based BB resonators with convex output couplers were presented in [11]. In both cases special attention was directed to the dependence of the output transverse profiles, the losses, and the modal frequency changes on the curvature of the output coupler and the cavity length.

In this paper we present a conventional (i.e., not axicon-based) confocal resonator configuration for the generation of BGBs. The mirror parameters are selected so as to form a Fourier transforming pair; when combined with an

* Corresponding authors. Tel.: +27 12 841 4188; fax: +27 12 841 3152.
E-mail addresses: ilitvin@csir.co.za (I.A. Litvin), aforbes1@csir.co.za (A. Forbes).

internal amplitude filter in the form of an annular aperture, the resonator is capable of supporting BGBs of various orders. In such a resonator the Gaussian field enveloping the Bessel field determines the radial modes, while the Bessel field determines the angular modes. These two functions together give rise to the potential for mode selection based on variable apertures inside the cavity. In Section 2 we introduce the resonator concept, and consider an analytical approach to understanding the mode behaviour inside the resonator. In Section 3 we analyze the resonator using the round trip Fourier transform, and then confirm the findings rigorously using the Fox–Li method in Section 4. We comment on the practicality of implementing this concept in Section 5.

2. Bessel–Gauss resonator concept

Bessel and Bessel–Gauss beams have been considered in detail elsewhere [1–4]. We briefly review the pertinent relationships to aid readability and clarity of the paper.

2.1. Bessel–Gauss beams

An ideal BB of order n can be described by [4]:

$$u_{\text{BB}}(r, z, \varphi) = A_0 \exp(ik_z z) J_n(k_r r) \exp(in\varphi), \tag{1}$$

where J_n is Bessel’s function of order n , k_z and k_r are the longitudinal and radial wavevectors with $k = \sqrt{k_r^2 + k_z^2} = 2\pi/\lambda$, with λ the wavelength of the electromagnetic field, and r, z , and φ are the radial, azimuthal and longitudinal co-ordinates, respectively. In practice a BB requires an infinite amount of energy to be generated, and so Bessel–Gauss Beams (BGBs) are used as an approximation to study the properties of BB over a finite extent.

A BGB is a BB described by Eq. (1) but modulated in amplitude by a Gaussian function, and can be expressed at its waist plane as

$$u_{\text{BGB}}(r, \varphi) = A_0 J_n(k_r r) \exp\left(-\frac{r^2}{w_0^2}\right) \exp(in\varphi), \tag{2}$$

where w_0 is the Gaussian $1/e^2$ radius at the waist. After propagating this field a distance z one can easily show that:

$$u_{\text{BGB}}(r, z, \varphi) = A_0 \frac{w_0}{w(z)} J_n\left(\frac{k_r r}{1 + iz/z_R}\right) \exp\left(-\frac{r^2}{w^2(z)}\right) \times \exp\left\{-\left[\frac{1}{w^2(z)} - \frac{ik}{2R(z)}\right](r^2 + k_r^2 z^2/k^2)\right\} \times \exp(in\varphi) \exp(i\phi(z)) \tag{3}$$

where $\phi(z) = k_r z - \arctan(z/z_R)$ and $R(z) = z[1 + (z/z_R)^2]$ is the radius of curvature of the Gaussian wavefront. The Gaussian $1/e^2$ beam radius at the distance z is described by $w(z) = w_0 \sqrt{1 + (z/z_R)^2}$.

The constant z_R represents the Rayleigh range of the Gaussian field, and is an indication of the distance over which the field may be considered collimated, given by

$$z_R = \frac{\pi w_0^2}{\lambda}.$$

Eq. (3) is valid when the starting BGB has a waist at $z = 0$, i.e., the wavefront is initially flat. It is equally valid to define the propagation of the BGB with a starting wavefront that has some curvature R , for example, by replacing Eq. (2) by

$$U_{\text{BGB}}(r, \varphi) = A_0 J_n(k_r r) \exp\left(-\frac{r^2}{w_0^2}\right) \exp(in\varphi) \exp\left(\frac{-ikr^2}{2R}\right). \tag{4}$$

We point this out since the field described by Eq. (4) will be shown to be one of the modes of the resonator described in this paper, and its propagation in the resonator will be studied in detail.

2.2. Fourier transforming resonator

When the geometric parameters of a resonator are chosen appropriately, the spherical curvature mirrors act as a Fourier transforming pair. In particular, if a stable resonator arrangement is employed with two concave mirrors having radius of curvature equal to the resonator length then the oscillating field will be Fourier transformed after each pass, so that after one complete round trip (two passes) the field is reproduced. The resonator we propose for this purpose has identical end mirrors, each of radius of curvature $R = 2f$, and separated along the optical axis by a distance $L = 2f$. A schematic of this resonator is shown in Fig. 1. Both mirrors M_1 and M_2 are of radius b , with M_1 having an additional obscuration in the form of a disk of radius a , creating an annular lossless zone between the disk edge and the mirror edge. The annular lossless zone is a significant factor in this resonator, and deserves further discussion. It has been shown previously [9] that when an intra-cavity lens is inserted into a planar–planar resonator such that the opposite mirrors are separated by one focal length from the lens (with the lens in the centre of the cavity), then a Fourier-transform relationship between the modal fields at the mirrors is established. Such a resonator was found to support Bessel–Gauss modes. It was pointed

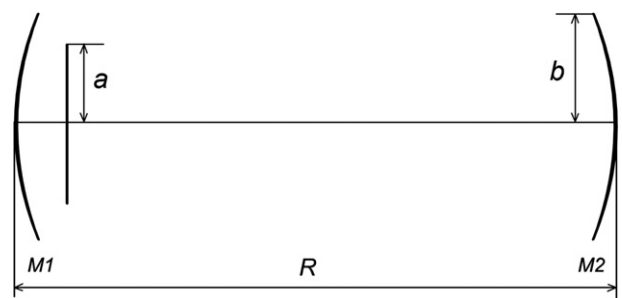


Fig. 1. Illustration of the Bessel–Gauss resonator. Mirror M_1 is obscured by a disk of radius d , thereby forming an annular lossless zone in the region $a < r < b$. Each mirror has a radius of curvature of $2f$ and they are separated by a distance of $2f$.

out that the modal discrimination of the resonator would be expected to be poor unless an annular aperture is employed at one of the mirrors. The resonator proposed in this study is analogous to such a cavity, but with spherical mirrors forming a Fourier-transforming pair. We will show in the sections to follow that the annular aperture size (a) and the mirror size (b) can be used as a mode selector where higher order Bessel fields have lower losses than lower order Bessel fields.

The field at mirror M_1 is uniquely defined by the lossless annular aperture, which if sufficiently narrow ($b-a \rightarrow 0$), will Fourier transform to a Bessel field. Since mirror M_2 is this Fourier transforming plane, the field distribution at M_2 would be the Bessel field. However the resonator we propose also supports Gaussian modes (we assume the dimensions of mirror M_2 are such that higher order Hermite–Gauss modes are eliminated) since the mirror curvatures match the curvature ($R(z)$) of the oscillating Gaussian field. So long as the Gaussian beam width encloses sufficiently many Bessel zeros, a well-defined annulus with an approximately Gaussian radial intensity distribution can be expected at mirror M_1 , in keeping with the concept of Bessel–Gauss fields as a superposition of conventional Gaussian beams with optical axes distributed uniformly on the surface of a cone [2]. Note that the resonator parameters (such as length and mirror curvatures) determine the Gaussian mode that oscillates, defining the radial modes of the resonator, while the apertures inside the resonator determine the angular modes that oscillate, as will be shown later. Both these modes play an important role in the analysis to follow.

2.3. Resonant modes

While the above description also serves as a heuristic argument for BGBs as modes of our resonator, it is instructive to show this more rigorously. We do so in two ways: firstly, we have shown numerically that BGBs of various orders are eigenmodes of this resonator. We pre-empt the discussion later by pointing out that a Fox–Li analysis of this resonator, starting from a random noise field, converges to various BGB orders, depending on the parameters of a and b . Fig. 2 shows intensity plots (a – e) of the zeroth order BGB during propagation through the resonator after the mode has reached a steady-state. The shaded area in the resonator drawing indicates the region where the BGB is in existence, with its largest spatial extent at mirror M_2 (position e), finally creating an annular ring at the opposite mirror (position a). This propagation is what is expected if the mode is a BGB. From the Fox–Li calculations one can also extract the phase of the BGB at the mirror (say mirror M_2 , for example). This is shown in Fig. 3, where the numerically calculated phase matches that of the mirror’s curvature exactly, as expected. Thus we can conclude that the field at mirror M_2 is indeed a BGB, with a wavefront matching the curvature of the mirror, i.e., $R = 2f$.

Secondly, we follow the approach detailed in [9] to test more rigorously if a BGB with a spherical wavefront is an eigenmode of this resonator. We start with a field just prior to reflection off mirror M_2 :

$$u_2(r, \varphi) = A_0 J_n(k_r r) \exp\left(-\frac{r^2}{w_2^2}\right) \exp(in\varphi) \exp\left(\frac{ikr^2}{4f}\right), \quad (5)$$

where w_2 is the beam size on mirror M_2 and is given by $w_2 = 3^{-\frac{1}{4}} \sqrt{\frac{8f}{k}}$. If the z axis is defined to be $z = 0$ at mirror M_2 , and positive to the left (in the direction of mirror M_1) then the Gaussian mode will propagate symmetrically about a waist centred at $z_0 = f$ with $w_0 = 3^{\frac{1}{4}} \sqrt{\frac{2f}{k}}$. We can determine the complete propagation of the field u_2 by using the Fresnel diffraction integral in the form [12]:

$$\begin{aligned} u(\rho, z) = & -i^{n+1} (k/z) \exp(ikz) \\ & \times \exp\left(\frac{ik}{2z} \rho^2\right) \int_0^\infty u_2(r) J_n\left(\frac{k\rho r}{z}\right) \\ & \times \exp\left(\frac{ik}{2z} r^2\right) \exp\left(-\frac{ik}{2f} r^2\right) r dr, \end{aligned} \quad (6)$$

where we have assumed that since the resonator is rotationally symmetric the modes are separable, and where we have made use of the well known integral representation of the Bessel functions:

$$\int_0^{2\pi} \exp(ix \cos \varphi) \exp(in\varphi) d\varphi = i^n 2\pi J_n(x).$$

The kernel of the integral includes phase modulation by mirror M_2 , which we treat as a thin lens of focal length f , followed by free space propagation through a distance z . The field at mirror M_1 will then be given by $u_1(\rho) = u(\rho, 2f)$, thus

$$\begin{aligned} u_1(\rho) = & -i^{n+1} A_0 (k/2f) \exp(i2kf) \exp\left(\frac{ik}{4f} \rho^2\right) \\ & \times \int_0^\infty \exp(-(r/w_2)^2) J_n(k_r r) J_n\left(\frac{k\rho r}{2f}\right) \\ & \times \exp\left(\frac{ik}{4f} r^2\right) \exp\left(\frac{ik}{4f} r^2\right) \exp\left(-\frac{ik}{2f} r^2\right) r dr \\ = & -i^{n+1} A_0 (k/2f) \exp(i2kf) \exp\left(\frac{ik}{4f} \rho^2\right) \\ & \times \int_0^\infty \exp(-(r/w_2)^2) J_n(k_r r) J_n\left(\frac{k\rho r}{2f}\right) r dr. \end{aligned}$$

By making use of the well known relation:

$$\begin{aligned} & \int_0^\infty \exp(-\sigma^2 x^2) J_p(\alpha x) J_p(\beta x) x dx \\ & = \frac{1}{2\sigma^2} \exp\left(-\frac{\alpha^2 + \beta^2}{4\sigma^2}\right) I_p\left(\frac{\alpha\beta}{2\sigma^2}\right), \end{aligned}$$

one can easily show that the field at mirror M_1 is given by

$$\begin{aligned} u_1(\rho) = & -iA_0 \frac{w_2^2}{4f} \exp(i2kf) \exp\left(-\frac{1}{4} w_2^2 \left[k_r^2 + \frac{k^2 \rho^2}{4f^2}\right]\right) \\ & \times J_n\left(\frac{ikk_r w_2^2}{4f} \rho\right) \exp\left(\frac{ik}{4f} \rho^2\right). \end{aligned} \quad (7)$$

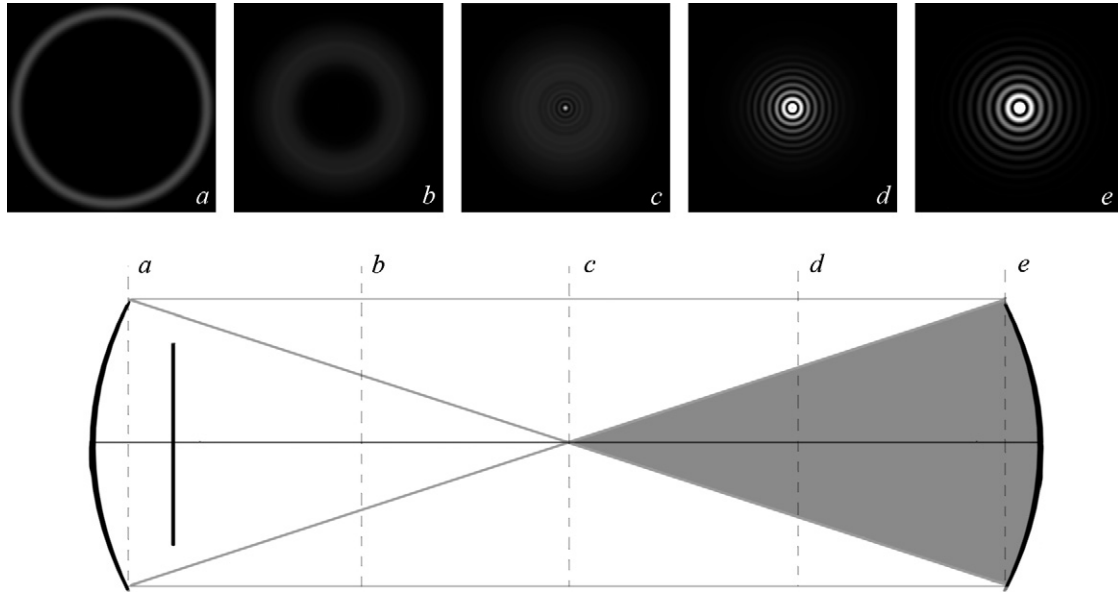


Fig. 2. The BGB is formed in the shaded region of the resonator, and changes in intensity as it propagates through this volume. Five intensity plots are shown corresponding to planes (a) through (e) within the resonator for the zeroth Bessel mode ($n = 0$). The starting mode was calculated using the Fox–Li algorithm with ten round trips, Fresnel number $N = 6$ and $a = \frac{5}{6}b$, and then propagated using Eq. (6).

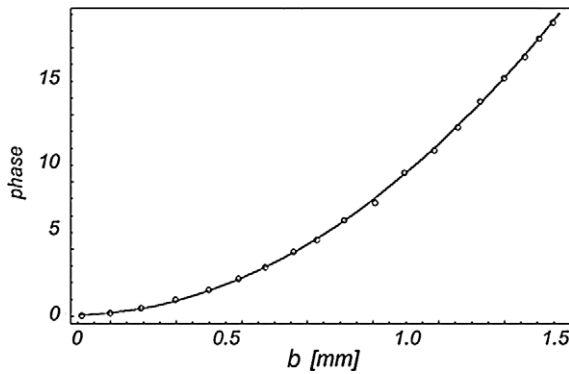


Fig. 3. Mirror phase as calculated from Eq. (7) (solid curve) as compared to the numerically calculated phase using the Fox–Li algorithm (data points).

Now we note that the required transfer function for mirror M_1 to support this mode can be found from:

$$t_{M1} = \frac{u_1^*}{u_1} = \exp\left(-\frac{ik}{2f}\rho^2\right),$$

where we have ignored constant phase terms. But this is precisely the phase of a spherical mirror of radius of curvature $R = 2f$, thus indicating again that the various orders of BGBs are modes of this resonator.

It is worth pointing out here an interesting aspect of this resonator. Conventionally one would consider the Fourier transform plane to be at $z = f$ and not $z = 2f$ when using a mirror of focal length f (or curvature of $2f$). However, the incoming field already has curvature Eq. (5), and thus the effective focal length of the mirror to a planar phase BGB field appears as $2f$:

$$\begin{aligned} u(r) &= A_0 J_n(k_r r) \underbrace{\exp\left(-\frac{r^2}{w_2^2}\right)}_{\text{BGB}} \underbrace{\exp\left(\frac{ikr^2}{4f}\right)}_{\text{lens}(f)} \underbrace{\exp\left(-\frac{ikr^2}{2f}\right)}_{\text{lens}(f)} \\ &= A_0 J_n(k_r r) \underbrace{\exp\left(-\frac{r^2}{w_2^2}\right)}_{\text{planar BGB}} \underbrace{\exp\left(-\frac{ikr^2}{2(2f)}\right)}_{\text{lens}(2f)} \end{aligned}$$

It is for this reason that the resonator mirrors are separated by a distance of $2f$.

The intensity profile at mirror M_1 is thus an annular beam modulated by a Gaussian envelope, while the intensity at mirror M_2 is the reconstructed BGB (Fourier transform of the annular field). If mirror M_2 is made partially transmitting, the resonator will emit various orders of Bessel–Gauss modes. Suitable collimating optics may be employed to correct the phase of the output beam if so desired.

3. Fourier optics analysis

We wish to consider the diffraction losses for each BGB order by applying the Hankel transform in Eq. (6) to propagate the field from mirror M_2 to M_1 , but with the limits of integration adjusted to $[0, b]$. The energy of the initial field is normalized such that the diffraction losses for the BGB of order n may be written as $\gamma = 1 - E_n$ where E_n is the energy at mirror M_1 after one pass. This single pass loss is representative of the steady state diffraction loss since the initial field chosen is already close to the stable mode under investigation. Because the field on mirror M_1 is annular-like for all mode numbers, showing very little discrimination between the modes, increasing or decreasing

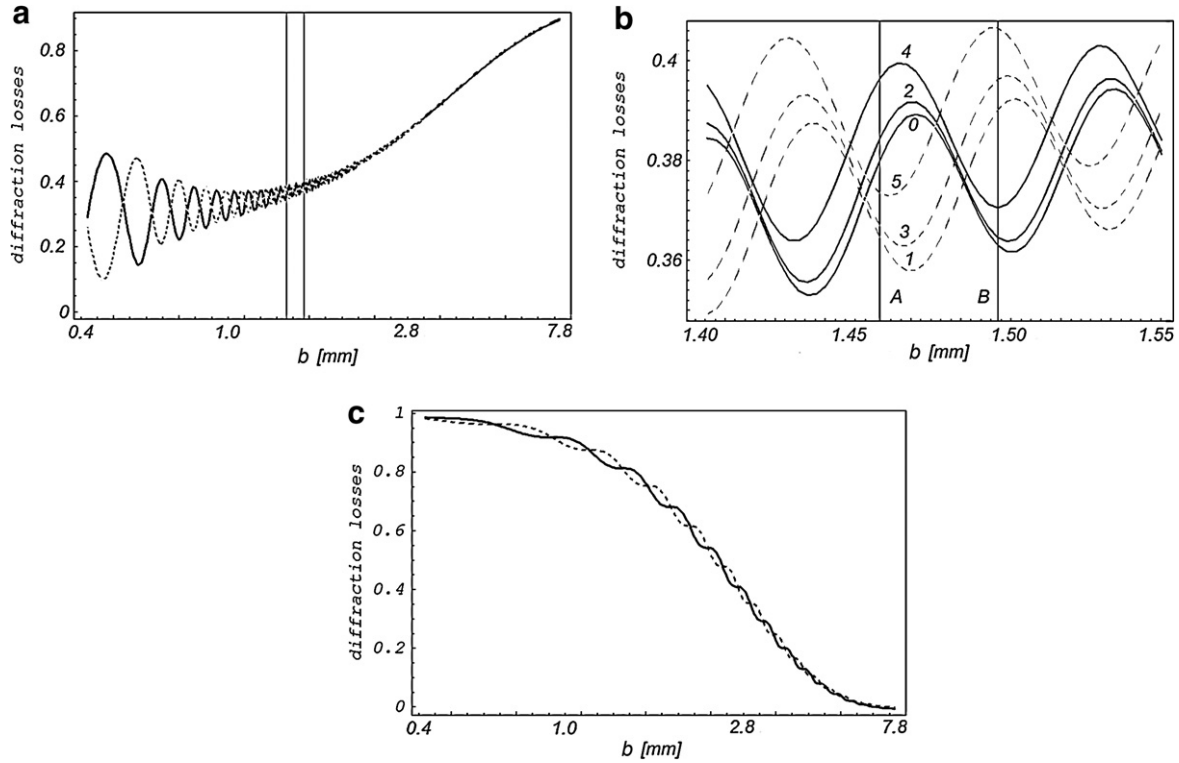


Fig. 4. The dependence of diffraction losses on radius b for the various orders of BGBs (even modes as solid curve, odd modes as dashed curve): (a) shows a general trend for the zeroth and first order mode of decreasing oscillation strength with increasing mirror radius due to the Gaussian envelope dominance when $b \gg w_2$. In this plot $a = 0.9b$, and thus the losses increase with b . A zoomed in area (between the vertical solid lines) is shown in (b), with the out of phase oscillations of the odd and even modes evident; (c) shows plot (a) but with a fixed in value.

the diaphragm radius a (or the mirror radius itself) will result in either increasing or decreasing losses for every BB order in a concomitant manner. Conversely, the BGB on mirror M_2 varies greatly with the Bessel function order. When the size of mirror M_2 is chosen so that b coincides with an intensity trough of the BGB, the diffractions losses will be minimized. In contrast, when b coincides with an intensity peak of the BGB, the diffractions losses will be maximized. This is easily noted if one considers that when $k_r r$ is large, Eq. (1) may be approximated as

$$u_{\text{BB}}(r, \varphi) = A_0 \sqrt{\frac{2}{\pi k_r r}} \cos\left(k_r r - \frac{2n+1}{4} \pi\right) \exp(in\varphi), \quad (8)$$

where we have dropped the piston phase term ($\exp(ik_z z)$). From this asymptotic approximation we observe that the amplitude of the field will oscillate with a cosine function for even orders of n , and as a sine function for odd orders of n , thus the even and odd orders are out of phase. This results in the diffraction losses of the modes on this mirror having an oscillatory character. One can also derive from Eq. (8) simple expressions for the radius b at which a particular order will have high or low losses:

$$b_{\text{HL}} = \frac{\pi(m + \frac{1}{2}n + \frac{1}{4})}{k_r}, \quad (9a)$$

$$b_{\text{LL}} = \frac{\pi(m + \frac{1}{2}n + \frac{3}{4})}{k_r}, \quad (9b)$$

where b_{HL} and b_{LL} are the values of b for high and low losses, respectively, m is an integer and n is the order of the BGB. For example, assume that an integer $m = m_0$ is chosen such that the J_0 function has high losses. Selecting an integer $m_1 = m_0 - 1$ will then ensure that the J_1 function has lower losses than the J_0 function. In general, if the integers in Eqs. (9a) and (9b) are chosen such that $m_0 - m_n = 1/2(n+1)$, then the losses in the J_0 will be larger than that of the J_n . Moreover, the decreasing losses for the even modes imply increasing losses for the odd modes, and vice versa.

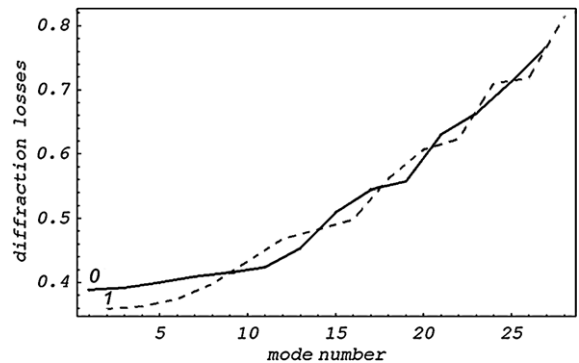


Fig. 5. The diffraction losses, as calculated by the Fourier approach, showing the zeroth order mode (0) with higher losses than some odd order modes (shown starting at 1, dashed curve). Calculations done at $b = 1.465$ mm corresponding to cross-section A of Fig. 4b.

In the limit that the enveloping Gaussian becomes much smaller than the mirror radius b , we expect this oscillatory behaviour to be suppressed by the zero asymptote of the Gaussian function, and at this point the radial modes completely determine the resonator behaviour.

In the analysis to follow the resonator parameters used for all calculations are: $f = 0.35$ m, $\lambda = 532$ nm, and $a = 0.9b$. Where other values have been used in calculations, it is clearly indicated so in the accompanying text.

The oscillatory nature of the diffraction losses for both odd and even modes, as described qualitatively earlier, is shown quantitatively in Fig. 4. Fig. 4 shows the convergence of the losses for all orders of odd and even modes when $b \gg w_2$, as is the norm in Fabry–Perot type cavities. The unusual feature of Fig. 4a, that the losses increase with increasing b , is due to the fact that a is also increasing according to $a = 0.9b$. Since an increase in obscuration at mirror M_1 increases losses for all modes, the net effect is

to increase the overall loss for each mode. Increasing b with a fixed in value, as is shown in Fig. 4c, results in an expected convergence to low loss for all modes. The results in Fig. 4a and c have been confirmed with a full Fox–Li analysis. Fig. 4b shows a zoomed-in section of Fig. 4a, with the section shown as vertical markers in Fig. 4a. The vertical cross-section A in Fig. 4b indicates a mirror radius at which some odd modes have higher losses than some even modes, while cross-section B shows the opposite. It is evident that at some values of b the lowest order BGB does not have the lowest losses; in general when the even modes have high losses, the odd modes have lower losses.

This fact is illustrated in Fig. 5 where it is evident that the BGB of zero order has higher losses than BGBs of order 1, 3, 5 and 7. By judicious selection of b one can again ensure that the zeroth order BGB has the lowest losses, as shown in Fig. 6, where even orders from 0 to 6 have lower losses than the first order BGB.

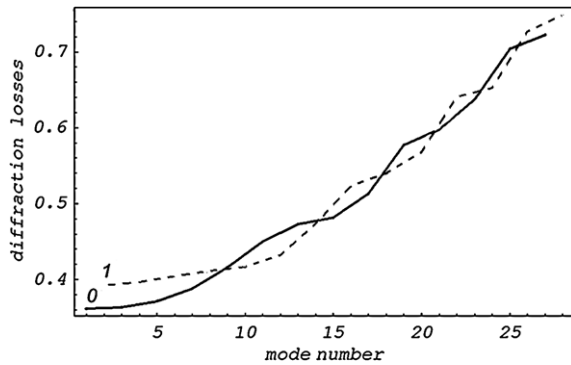


Fig. 6. The zero order mode (0) now has the lowest losses, with a clear out-of-phase oscillation in the loss for odd (starting at 1, dashed curve) and even (starting at 0, solid curve) modes. Calculations done at $b = 1.50$ mm corresponding to cross-section B of Fig. 4b.

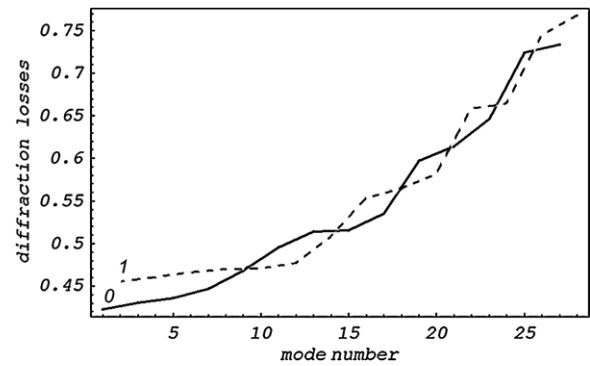


Fig. 7. The dependence of the diffraction losses per round trip on the mode number, as calculated using the Fox–Li method. Odd modes are shown starting at 1 in the dashed curve, while even modes are shown starting at 0 in the solid curve. The results are in very good agreement with those shown in Fig. 6.

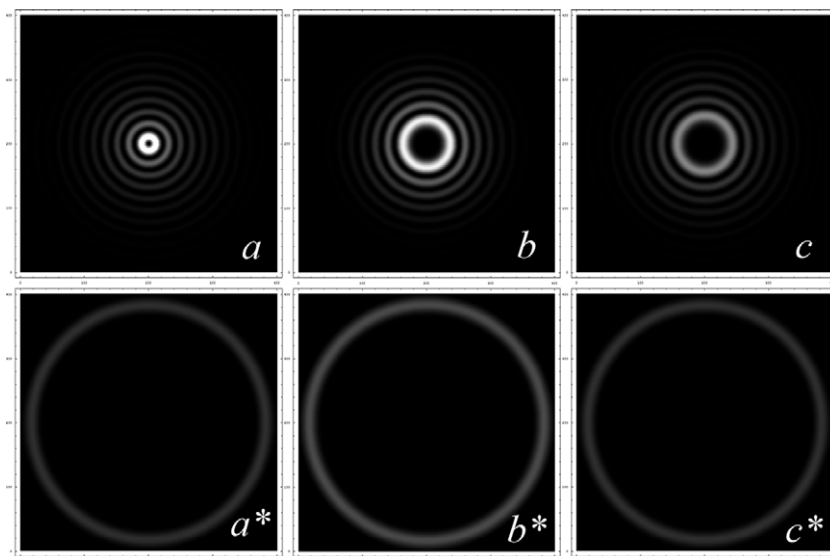


Fig. 8. Examples of the calculated BGBs with their corresponding Fourier transforms: (a) J_1 , (b) J_5 and (c) J_6 Bessel orders.

We also note from Fig. 5 that the oscillatory nature of the mode losses is suppressed at high mode numbers (e.g., beyond 20); this is due to the nature of the oscillations in the Bessel functions themselves, where the approximation Eq. (8) becomes valid at radii that increase with the Bessel order.

4. Fox–Li analysis

To confirm the results of Figs. 5 and 6, we consider a full wave optics analysis using the Fox–Li method [12]. The calculation was performed with $b = 1.50$ mm and the results are shown in Fig. 7. Comparison of Figs. 6 and 7 clearly shows that the approach of the previous section is in good agreement with the full wave optics analysis. The oscillatory nature of the losses for the odd and even orders is evident in both trends, showing excellent qualitative agreement, while there is very close quantitative agreement in the calculated losses.

The propagation of the zeroth order BGB is shown in Fig. 2, while some examples of the resulting steady state fields and their Fourier transforms are shown in Fig. 8. The propagation characteristics, as well as the Fourier transform of the fields confirms that these are indeed BGBs. The fact that the losses for various orders may be to some extent controlled in this resonator opens the way for selection of higher order BGBs.

5. Conclusion

We have analyzed a Fourier transforming type resonator that generates BGBs of various orders as an output. The losses of these modes have revealed an oscillatory nature, which suggests that the lowest order BGB may not necessarily have the lowest loss. This can be understood in terms of odd and even modes by using the asymptotic approximation to the Bessel function. The analytical theory indicates that specific resonator conditions would be necessary to ensure that the lowest loss can be obtained in the lowest order mode. The general rule for Fabry–Perot type resonators, which explains that the lower order modes have lower loss is not necessarily correct in this particular resonator. The simplified Fourier approach was validated by a more rigorous Fox–Li analysis which confirmed the findings.

We also wish to point out some practical implications in generating BGBs from such a resonator. Firstly, since the resonator consists of only conventional optical elements (spherical curvature mirrors and circular apertures) no special alignment techniques are required. Secondly, due to the fact that the order of the BGB of lowest loss is determined only by the diameter of mirror M_2 , a simple variable aperture (iris) at the position of mirror M_2 should suffice as a mode selector in much the same way that the various Hermite–Gauss modes may be selected by suitable

aperture choice. This paper has dealt mostly with loss aspects of the modes, but the issue of optical gain requires a mention. As illustrated in Fig. 2, the BGB does not fill the entire cavity, and is most pronounced near mirror M_2 . This suggests that the gain medium in a practical system would have to be placed near mirror M_2 and have a larger cross-sectional area and a comparatively short length. For example, if the laser had a solid state gain medium, there would be benefit in using a disk-like gain medium rather than a rod to maximize the mode volume inside the gain region. It would also be possible to amplify the field near mirror M_1 , but this would require an annular gain region, which while not impossible, may not be easily implemented in practice.

Finally, the typical aperture dimensions found in this study would not deter practical implementation of such a resonator concept.

Acknowledgement

We would like to thank Dr A. N. Khilo for useful discussions and advice.

References

- [1] J. Durnin, *J. Opt. Soc. Am. A* 4 (1987) 651.
- [2] J. Durnin, J.J. Miceli, J.H. Eberly, *Phys. Rev. Lett.* 58 (1987) 1499.
- [3] J. Durnin, J.H. Eberly, *Diffraction Free Arrangement*, Patent No. 4887885, December 19, 1989.
- [4] D. McGloin, K. Dholakia, *Contemp. Phys.* 46 (2005) 15.
- [5] J.K. Jabzynski, *Opt. Commun.* 77 (1990) 292.
- [6] J. Rogel-Salazar, G.H.C. New, S. Chavez-Cerda, *Opt. Commun.* 190 (2001) 117.
- [7] A.N. Khilo, E.G. Katranji, A.A. Ryzhevich, *J. Opt. Soc. Am. A* 18 (2001) 1986.
- [8] C.L. Tsangaris, G.H.C. New, J. Rogel-Salazar, *Opt. Commun.* 223 (2003) 233.
- [9] P. Paakkonen, J. Turunen, *Opt. Commun.* 156 (1998) 359.
- [10] J.C. Gutierrez-Vega, R. Rodríguez-Masegosa, S. Chavez-Cerda, *J. Opt. Soc. Am. A* 20 (2003) 2113.
- [11] R.I. Hernandez-Aranda, S. Chavez-Cerda, J.C. Gutierrez-Vega, *J. Opt. Soc. Am. A* 22 (2005) 1909.
- [12] A.G. Fox, T. Li, *Bell Syst. Tech. J.* 40 (1961) 453.



Igor A. Litvin received his Diploma (Physics) in 2002 from Belarus State University in the field of Physical Optics. He has been a researcher at the National Academy of Science of Belarus till 2005, at which point he joined the National Laser Centre (NLC) of South Africa as an invited scholar. He is presently enrolled for a PhD (Physics) at the University of Stellenbosch (South Africa). His main research areas are mathematical optics, resonators, turbulence optics, wave guides, and intra and extra cavity laser beam shaping.

He is with the CSIR National Laser Centre, P.O. Box 395, Pretoria 0001, South Africa and the Laser Research Institute, University of Stellenbosch, Stellenbosch 7602, South Africa (phone: +27 12 8412368; fax: +27 12 8413152; e-mail: ilitvin@csir.co.za).



Andrew Forbes received his BSc (Physics/Mathematics) in 1990, BSc Hons (Physics) in 1991 and PhD (Physics) in 1998 from the University of Natal, Durban (South Africa). His doctoral thesis considered photo-thermal effects due to high power laser beams. He has spent several years working as an applied laser physicist, first for the South African Atomic Energy Corporation on high power lasers for the MLIS process for Uranium enrichment, and then later on gas lasers for laser ultrasonic applications. He is presently a

Principal Researcher at the CSIR National Laser Center (Pretoria, South Africa) and is the Research Group Leader for the Mathematical Optics

group. His research interests include laser beam propagation, wavefront control for laser beam shaping and laser resonator analysis and design.

He is chair of the SPIE Laser Beam Shaping conference, and is an active member of SPIE. He is also a member, and secretary, of the South African Institute of Physics 'Laser Optics and Spectroscopy' specialist group.

He is with the CSIR National Laser Centre, P.O. Box 395, Pretoria 0001, South Africa and a member of the School of Physics, University of KwaZulu-Natal, Private Bag X54001, Durban 4000, South Africa (e-mail: aforbes1@csir.co.za).